Tribology Transactions, 58: 207-214, 2015

ISSN: 1040-2004 print / 1547-397X online
DOI: 10.1080/10402004.2014.960540

stle
Society of Tribologists and Lubrication Engineers

Friction Reduction Benefits in Valve-Train System Using IF-MoS_2 Added Engine Oil

M. SGROI,[1] F. GILI,[1] D. MANGHERINI,[1] I. LAHOUIJ,[2] F. DASSENOY,[2] I. GARCIA,[3] I. ODRIOZOLA,[3] and G. KRAFT[4]
[1]Centro Ricerche Fiat, Group Materials Labs 10043, Orbassano, Italy
[2]Ecole Centrale de Lyon, LTDS 69134, Ecully, France
[3]Materials Division, IK4-CIDETEC Research Centre, 20009 Donostia–San Sebastián, Spain
[4]FUCHS Europe Schmierstoffe, 68169 Mannheim, Germany

The development of new advanced lubricants is a key factor for the production of cleaner and more durable internal combustion engines. New improved antifriction and antiwear additives are required. The inclusion of nanoparticles known as solid lubricants (MoS_2 and WS_2 inorganic fullerenes) in fully formulated engine oils could help to improve the performance of the lubricant and of the engine.

The AddNano Consortium, partially funded by the European Commission, investigated the possibility of including inorganic fullerenes in the formulation of engine oils. MoS_2 nanoparticles integrated in the additive package of an SAE 5W30 engine oil showed a 50% reduction in the coefficient of friction in tribological lab-scale experiments. The nano-oil was formulated by modifying the additive package in order to stably disperse the nanoparticles and avoid counterproductive interactions with the other components of the package (antifoam, antioxidant, detergents, antiwear and antifriction additives).

In the present work, characterization of the nanolubricants on a bench test simulating the real tribological conditions encountered in the valve-train of a diesel engine is reported. transmission electron microscopy (TEM) and X-ray photoelectron spectroscopy (XPS) were used to characterize the nanoparticles and the rubbed surfaces.

KEY WORDS

Inorganic Fullerenes; Nanolubricant; Friction Reduction; X-Rays Photolectron Spectroscopy

INTRODUCTION

The development of new advanced lubricants is a key factor for the production of cleaner and more durable internal combustion engines. The improvement in performance and efficiency of modern engines is mainly related to optimization of the combustion process, but this requires, in parallel, improved materials able to sustain extreme working conditions. In this scenario, new lubricants and coatings for engine components are of fundamental importance. The engine oil has an important role in the improvement of fuel economy due to the reduction in friction and has a strong impact on the durability of mechanical components and on the behavior of the emission after-treatment system. The roadmap on the development of new engine oils foresees the progressive reduction in the viscosity of the lubricant, in order to reduce the losses in the elastohydrodynamic regime. Consequently, new improved antifriction and antiwear additives are required to protect the mechanical components during cold start-up when a boundary lubrication regime can occur. Moreover, exhaust catalysts tend to become poisoned by elements that are components of the additives and the mesh structure of diesel particulate filters can become irreversibly blocked by ashes related to the additive package of the lubricant. For this reason, lubricants that contain lower amounts of ash-giving components are being developed for modern diesel engines.

Ash derived from lubricant additives is composed primarily of zinc and calcium, in the form of sulfates, phosphates, and oxides. Zinc is found in disproportionately high amounts in the after-treatment systems in comparison to other ash-giving, lubeborn elements like calcium. Due to the potentially higher concentrations of zinc additives in the raw emissions, they probably have more deleterious effects on the after-treatment system compared to other metal-containing, ash-giving additives; for example, those based on calcium. Based on these considerations, a Zn-free lubricant was chosen for the present work.

In this scenario, the inclusion of nanoparticles known as solid lubricants (MoS_2 and WS_2 inorganic fullerenes; Cizaire, et al. *(1)*; Joly-Pottuz, et al. *(2)*; Lahouij, et al. *(3)*; Yadgarov, et al. *(4)*; Verma, et al. *(5)*; Gullac and Akilin *(6)*; Mosleh and Ghaderi *(7)*) in a fully formulated engine oil could help to improve the performance of the lubricant and of the engine.

The AddNano Consortium, partially funded by the European Commission, investigated the possibility of including inorganic fullerenes and similar particles in the formulation of engine oils and greases.

MoS_2 nanoparticles integrated in the additive package of a Fuchs' engine oil showed a 50% reduction in the coefficient of friction in tribological lab-scale experiments (Cizaire, et al. *(1)*). The nano-oil was formulated by modifying the additive

Manuscript received March 25, 2014
Manuscript accepted August 27, 2014
Review led by Elaine Yamaguchi
Color versions of one or more of the figures in the article can be found online at www.tandfonline.com/utrb.

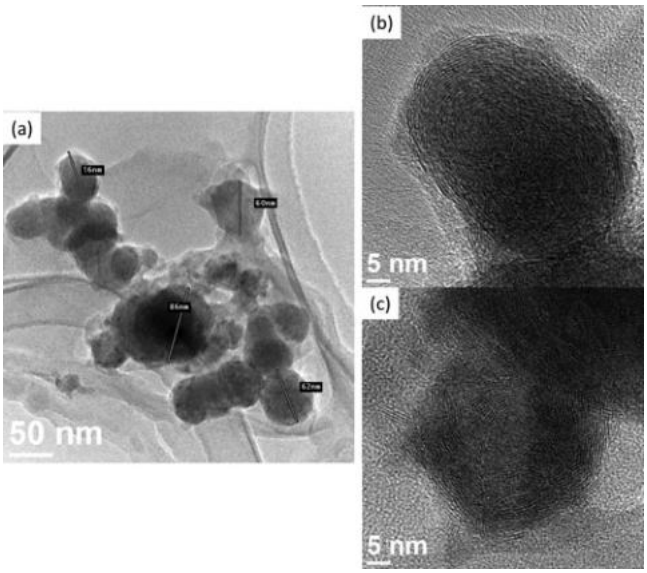

Fig. 1—High-resolution TEM images of IF-MoS_2 nanoparticles.

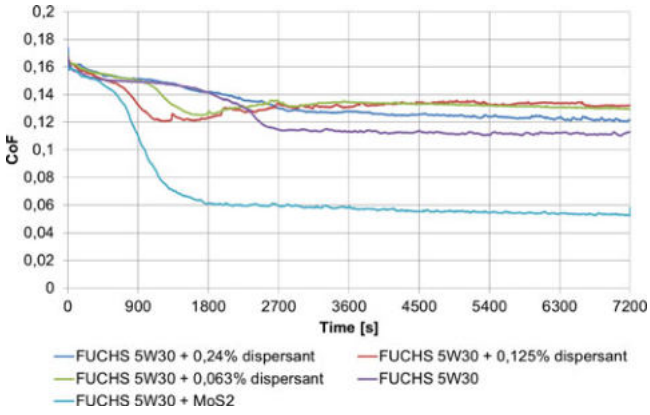

Fig. 2—Effect of the concentration of dispersing agents on the coefficient of friction measured in SRV oscillating tests. The results show that the coefficient of friction is not significantly modified with respect to the reference oil. SRV conditions: stroke 4 mm, frequency 20 Hz, load 150 N, temperature 130°C.

package in order to stably disperse the nanoparticles and avoid counterproductive interactions with the other components of the package (antifoam, antioxidant, detergents, antiwear and antifriction additives).

In the present work, characterization of the nanolubricants on a bench test simulating the real tribological conditions encountered in the valve-train of a diesel engine is reported.

Transmission electron microscopy (TEM) and X-ray photoelectron spectroscopy (XPS) were used to characterize the nanoparticles and the rubbed surfaces. XPS is a powerful technique to investigate the chemical composition of tribolayers and was recently applied by Morina, et al. *(8)* to investigate tribofilms containing molybdenum.

EXPERIMENTAL DETAILS

Nanoparticles and Lubricating Oils

The MoS_2 nanoparticles were synthetized by IK4-CIDETEC using a low-cost wet chemistry route that can be easily scaled up for industrial production. Further details are not given here due to confidentiality reasons. Prior to mixing nanoparticles with oil, MoS_2 nanoparticles were characterized. The typical size distribution of the IF-MoS_2 nanoparticles is between 50 and 100 nm. The morphology determined in high-resolution TEM observations (Fig. 1) is of nearly spherical IF-type with concentric nested layers showing a considerable amount of point defects and grain boundaries, thereby proving their amorphous character.

Based on XPS analysis carried out on the IF-MoS_2 powder, the ratio between sulfur and molybdenum was estimated to be 1.85 (see Table 1).

A concentrated dispersion of particles in base oil with two types of dispersants was prepared using a stirred bead mill following the procedure described in Utomo, et al. *(9)*. The dispersants are needed to avoid aggregation and settling of the solid phase.

This preconcentrate was subsequently blended into the final formulation, giving a much lower particle concentration on the order of 0.1 to 1%.

The additive package of the nanolubricant was adapted to obtain a stable dispersion by modifying the typology and concentration of dispersing agents. The effect of different dispersant concentrations was investigated by a series of Schwingung Reibung Verschleiβ (SRV) oscillating tests using piston ring segments and cast iron disc samples as a counterpart simulating the cylinder liner. As can be observed in Fig. 2, minor differences were detected in the coefficient of friction time history corresponding to three different dispersant concentrations, all of them comparable to reference Fuchs 5W30 oil and noticeably far from Fuchs 5W30 + MoS_2, in which the friction reduction contribution of the considered nanoparticles was noticed for the first time.

In addition to the different concentrations of dispersants and the presence of nanoparticles, the nanolubricant was identical to the reference oil. The stability of the nanolubricant was confirmed by settlement tests performed over a period of one year.

The tested samples and their characteristics are reported in Table 2. As expected, the presence of nanoparticles, due to the low concentration, does not modify the viscosity and rheological properties of the fluids.

TABLE 1—XPS QUANTIFICATION OF IF-MoS_2 POWDER

	Elemental Composition (at%)			
Elements	C1s	O1s	S2p	Mo3d
Atomic%	40	20	26	14

TABLE 2—DENOMINATION AND PROPERTIES OF TESTED NANOLUBRICANTS SAMPLES

Sample	Viscosity Grade	Kinematic Viscosity
Fuchs 5W30	5W30	60.04 at 40°C, 10.18 at 100°C
Fuchs 5W30 + MoS_2	5W30	60.11 at 40°C, 10.18 at 100°C

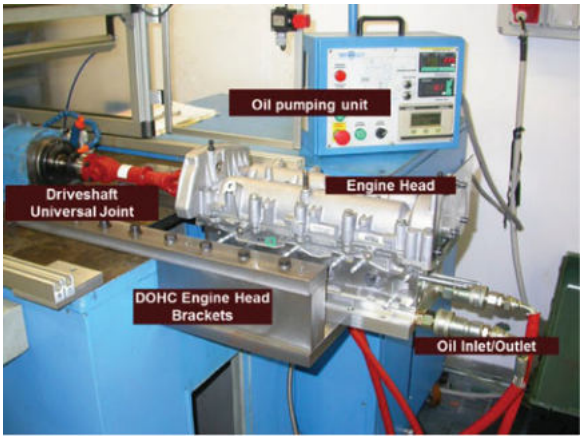

Fig. 3—Motored head test rig.

Engine Head Tests: Test Rig and Procedure

The friction reduction potential of the nanolubricant was evaluated using a motored engine head rig as shown in Fig. 3. A cylinder head from a 1.6-L, 16-V, four-cylinder in-line diesel engine equipped with a roller-finger follower (RFF) valve-train system was used for the test. The cylinder head was mounted on a supporting bench and one of the two camshafts was driven by an electric motor. An in-line 50 Nm torque transducer was used to measure the resistant torque. The engine oil was heated in an external unit and pumped into the engine inlet at 110°C to be circulated in the head channels and lubricate the valve-train system. The lubricant pressure in the head was set at 3 bar. The test duration was 250 h corresponding to a covered running distance of 60,000 km; rotational velocities of the driving shaft in the range 1,000–4,000 rpm were applied according to an 8 h 20 min predefined testing cycle (Fig. 4), repeated 30 times.

Surface Analysis

Chemical analysis of the tribofilms was performed by XPS. With a probing depth of a few nanometers (5 nm), this technique is the most convenient for surface analysis and wear scar characterization. A PHI Quantum 2000 system, with a high-power monochromatic Al K_α X-ray source (hv = 1,486.68 eV) was used.

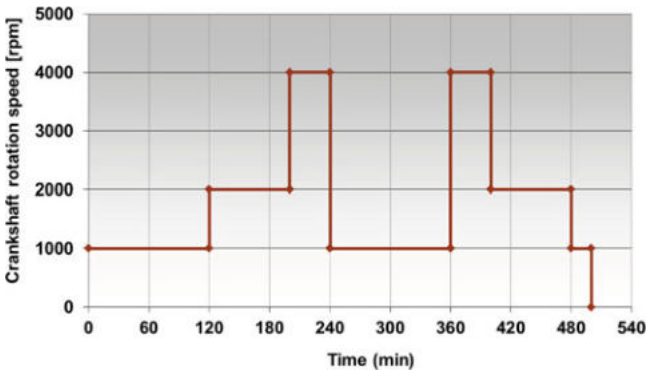

Fig. 4—Motored head test cycle.

The X-ray beam was focused in the wear scar and an area of 100 μm * 100 μm^2 was probed. In a typical XPS analysis, a survey scan is first recorded in order to identify the chemical elements present in the probed area. Then, high-resolution spectra of selected peaks (characteristics of each element) are performed in order to get complete information on the chemical composition (chemical bindings) of the tribofilm. Spectra were recorded in spatial mode. The deconvolution of these peaks allowed identification of the different chemical species. Chemical analyses as a function of depth were also performed. The argon etching was performed using 2 KeV Ar ions in an area of 2 × 2 mm, calibrated to an SiO_2 etching rate of ~2 nm/min. The pass energy for the survey and long scans was 187.4 and 23.5 eV, respectively. The resolution of the XPS was 0.3 eV, and the position of the C1s peak (284.8 eV) was considered as the reference for charge correction.

The XPS analyses were performed in several areas, inside and outside the wear track region, in order to verify the repeatability of the results.

Multi Pack software was used to analyze the XPS spectra obtained from long scans. Quantitative analyses of the peaks were performed using peak area sensitivity factors. An XPS handbook (Moulder, et al. *(10)*) and online databases (www.lasurface.com) were used to attribute the binding energies to chemical species. The peak area ratio (difference between binding energies of the doublets and full-width at half maximum) were constrained in order to obtain information with the most appropriate chemical meaning. A Shirley background was taken into account for the data process.

RESULTS

Tribology

In Fig. 5, the average value of the average torque versus time history is reported for Fuchs 5W30 (blue curve) and Fuchs 5W30 + MoS_2 (red curve) lubricants. The frictional benefit of the nanolubricant (red curve) was proven at all selected speeds, in particular, for low (1,000 rpm) and medium (2,000 rpm) speeds, mainly associated with boundary and mixed lubrication regimes. During the test, a significant decrease in the torque ascribable to the growth on the contacting surfaces of a beneficial low friction tribolayer was detected.

A detailed analysis of the output data (Fig. 6) showed that in the first 8 h of testing the nanolubricant (red curve) was more effective in reducing friction at higher speed regimes (2,000 and 4,000 rpm) where mixed lubrication (ML) and hydrodynamic lubrication (HL) lubrication conditions prevail.

During the second cycle (hours 8–16), the nanolubricant competed with the standard lubricant at low speed in the first part of cycle. Then a clear friction advantage in all lubrication regimes was noted for the nano-oil.

Finally, in the very last part of the test (hours 242–250), the nanolubricant showed the lowest friction torque at all lubrication regimes; in particular, at low and medium speeds the torque values were uniform and set in the range between 1.4 and 1.6 Nm.

The reduction in the absorbed torque in the boundary and mixed regimes was thus attributed to the buildup of a low friction film due to the exfoliation of IF-MoS_2 nanoparticles occurring on

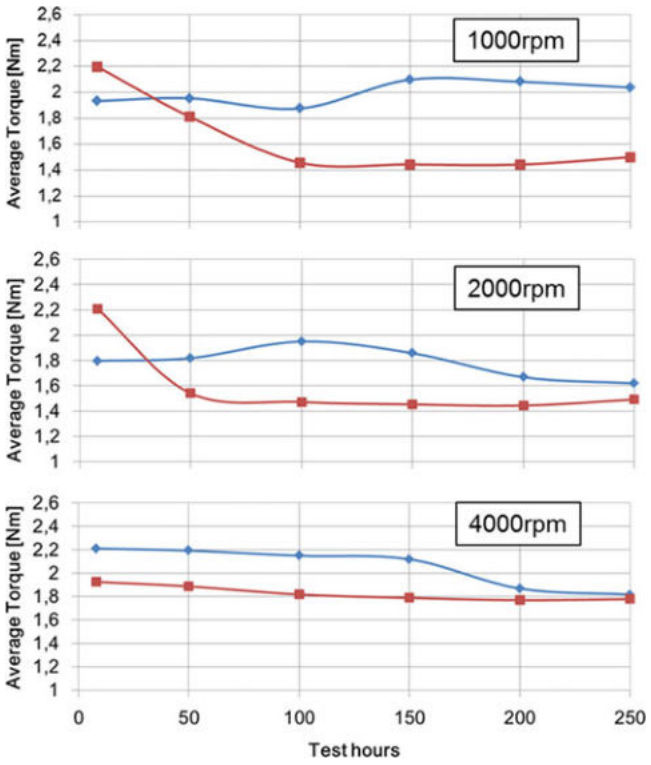

Fig. 5—Time history of the average torque at 1,000, 2,000, and 4,000 rpm.

the sliding surfaces of the valve-train components. Because an increase in the frictional benefit was observed from the beginning through the end of the test, it was also hypothesized that a certain amount of time was needed to generate the tribolayer, which, afterwards, was effective up to the end of the test.

Surface Analysis

XPS analyses were performed inside and outside the contact areas of carbonitrided steel RFFs, after motored head tests carried out with Fuchs 5W30 and Fuchs 5W30 + MoS_2 lubricants. XPS survey scans and XPS quantification are reported in Fig. 7 and Table 3, respectively.

XPS spectra recorded outside the wear area showed no additive-derived elements except the calcium (Ca) peak, which comes from the detergent adsorbed on the surface. Carbon and oxygen were also found outside the wear track.

Inside the wear track and for the engine test carried out with Fuchs 5W30, calcium, phosphorus, and sulfur were detected as well as an iron peak.

Phosphorus and calcium are detected in the tribofilms formed from the Fuchs 5W30 reference oil and the Fuchs 5W30 + MoS_2 oil. The results clearly indicate that the presence of the antiwear additive and detergent in the formulation do not affect the friction modifier properties of the MoS_2 nanoparticles. The interaction between metal disulfide nanoparticles (WS_2) and phosphorus-based antiwear additives was recently investigated by Jenei, et al. *(11)*. The authors performed friction tests at 40°C in the presence of different additives used for engine oil formulations, including zinc dialkyl dithiophosphate antiwear additive and detergent. No antagonist effects between the nanoparticles

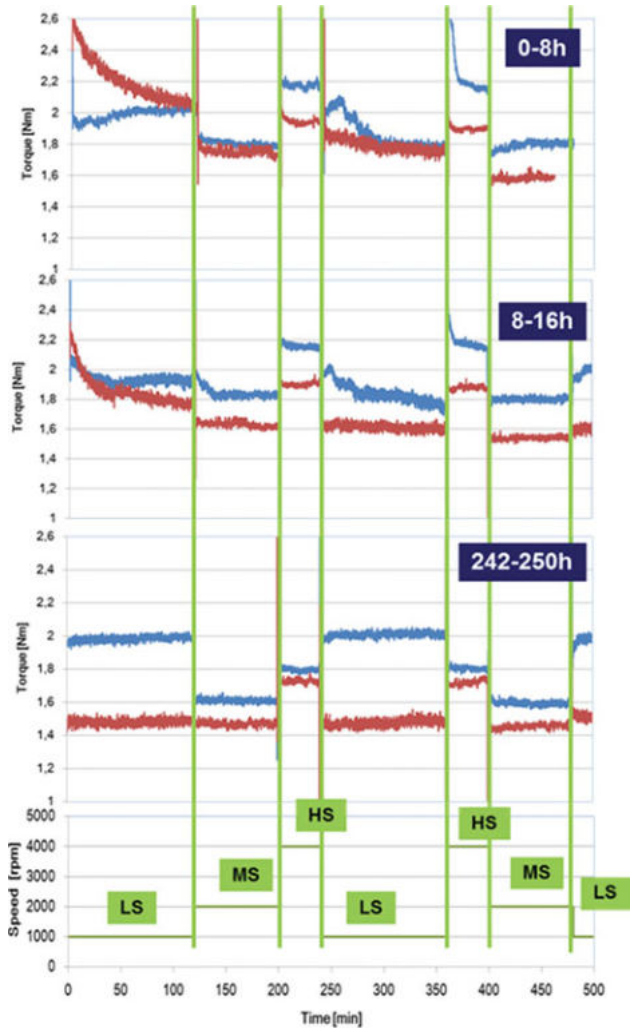

Fig. 6—Torque history details (LS: low speed, MS: medium speed, HS: high speed).

and the different additives were found, and synergetic effects (in terms of friction or wear) were also sometimes observed. Even if no detailed chemical analysis of the tribofilm was done, Jenei, et al. *(11)* showed that the final composition of the tribofilm was influenced by the presence of the other additives. These results

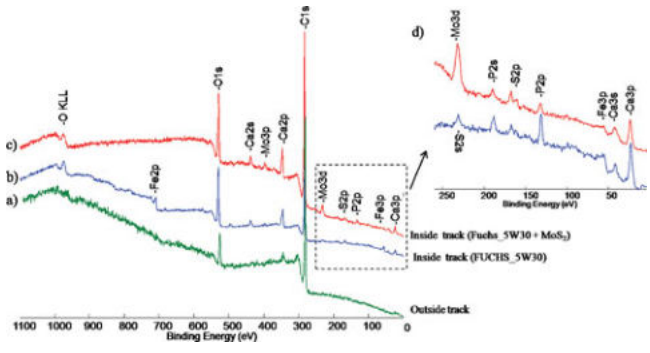

Fig. 7—XPS survey scan recorded (a) outside the wear track, (b) inside the wear track lubricated with Fuchs 5W30 oil, and (c) inside the wear track lubricated with Fuchs 5W30 + MoS_2.

TABLE 3—XPS QUANTIFICATION OF TRIBOFILMS OBTAINED WITH FUCHS 5W30 AND FUCHS 5W30 + MoS_2

Elemental Composition (at%)	Outside Tribofilm	Tribofilm (Fuchs 5W30)	Tribofilm (Fuchs 5W30 + MoS_2)
C1s	73	50	49
O1s	23	37	35
Ca2p	3	8	9.5
P2p	0.5	2	1.6
S2p	0.5	1	2.3
Mo3d	0	0	2.1
Fe2p	0	2	0

are consistent with those obtained in this work with a fully formulated oil containing nanoparticles. Ca, P, and MoS_2 nanoparticles contribute to the formation of the tribofilm without any antagonist effects and the friction reducing properties of the nanoparticles are preserved.

The observation of the Fe peak suggests that despite decomposition of the antiwear additive and the formation of a protective tribofilm made of sulfur and phosphorus, part of the carbonitriding treatment was removed during the engine test. Another option can be the presence of iron oxide particles embedded in the tribofilm and produced during the friction test. This could therefore explain the detection of Fe in the XPS spectra.

For the test done with Fuchs 5W30 + MoS_2, XPS reveals the presence in the wear track of an additional element compared to those detected with Fuchs 5W30. Molybdenum coming from the MoS_2 nanoparticles is detected. XPS quantifications (Table 3) show that the tribofilm formed with Fuchs 5W30 + MoS_2 contains two times more sulfur than the tribofilm formed with Fuchs 5W30. This means that the molybdenum as well as part of the sulfur detected in the tribofilm formed with Fuchs 5W30 + MoS_2 came from the IF-MoS_2 nanoparticles added to Fuchs 5W30. It was also found from the XPS survey scan (Fig. 7) that in contrast to Fuchs 5W30, an Fe2p peak was not detected in the Fuchs 5W30 + MoS_2 tribofilm. Considering that XPS is a surface-sensitive technique, it can be concluded from these observations that the tribofilm obtained with Fuchs 5W30 + MoS_2 looks thicker than the tribofilm obtained with Fuchs 5W30. The absence of Fe in the XPS spectrum could also be explained by the absence of wear during the engine test.

In order to investigate the chemical composition of the tribofilm obtained with Fuchs 5W30 + MoS_2 in depth, XPS depth analyses were carried out by combining a sequence of ion gun etch cycles with XPS measurements. Therefore, the chemical quantification of the tribofilm was followed from the uppermost surface and after 0.2, 1, 4, 10, and 18 min of etching as shown in Table 4.

Table 4 shows that the carbon content decreases from the first cycle of etching compared to the uppermost surface of the tribofilm. This indicates that the carbon detected before the beginning of etching is due to contamination of the tribofilm by carbon. Thus, after removing the carbon contamination, the real composition of the tribofilm formed from the additives can be measured.

The XPS quantification of the tribofilm as a function of depth showed that the carbon content continues to decrease progressively with etching time, and the oxygen content remains stable until 10 min of etching and then decreases drastically after 18 min. In parallel, the iron content increases progressively as a function of depth from 1.5% after 0.2 min of etching to 71% after 8 min of etching.

With regard to the additive-derived elements, the amount of calcium remains stable and high after 10 min of etching, whereas the phosphorus decreases progressively with depth so that it is no longer detected after the last cycle of etching. In addition, molybdenum and sulfur were detected throughout the etching time. After 10 min of etching, their percentages remain relatively stable and higher than those measured before etching. This confirms the contribution of the MoS_2 nanoparticles added to Fuchs oil to the formation of a thick tribofilm with improved antifriction and possibly antiwear properties.

In order to better understand the contribution of the nanoparticles to the formation of the protective tribofilm, the chemical state of the tribofilm formed with Fuchs 5W30 + MoS_2, the binding energies, the chemical states, and quantification of the fitted (Mo3d, S2p, C1s, O1s, and Fe2p) peaks collected from the uppermost surface of the tribofilm and after 0.2, 1, 4, 10, and 18 min of etching are given in Table 5.

Furthermore, the fitted S2p and Mo3d peaks obtained from the uppermost surface and after 0.2, 4, 10, and 18 min of etching were compared to those obtained from the IF-MoS_2 nanoparticles as shown in Fig. 8. The chemical states of Mo and S were similar after 1 and 4 min of etching.

Figure 8 shows that molybdenum and sulfur were found in different chemical environments in the powder and the tribofilm. With regard to the XPS spectra recorded from the IF-MoS_2 powder, the sulfur $S2p_{3/2}$ is composed of a main peak at 161.1 eV corresponding to sulfur (67%), a peak at 162.4 eV corresponding to the S-Mo bond of IF-MoS_2 nanoparticles (20%), and a small contribution at 167.8 eV attributed to S-oxide bonds (13%). The $Mo3d_{5/2}$ is composed of four peaks, a main peak at 228 eV corresponding to elemental molybdenum (47.9%), a peak at 229.1 eV (27.5%) corresponding to Mo−S bond of IF-MoS_2 particles, a peak at 231.3 eV corresponding to MoO_yS_x (16%), and a small contribution at 232. 9 eV attributed to Mo-oxide bonds (MoO_3; 8.5%). The presence of sulfide and elemental molybdenum in the powder could be related to the synthesis processes, and the presence of S−O and Mo−O bonds could be explained by soft oxidation of the powder.

XPS spectra recorded from the uppermost surface of tribofilm are different from those recorded on the powder. Only small contributions of sulfur and molybdenum are observed, respectively, at 161.8 eV (19%) and 229.1 eV (5%), corresponding to Mo−S bonds. Moreover, an increase in the intensity of the Mo−O and S−O bonds can be observed for the tribofilm.

With regard to the sulfur, a new contribution is observed at 163 eV, corresponding to S−C and/or S-S bonds (25%). The two other contributions of sulfur at higher energy were attributed to S-oxide bonds (60%). With regard to the molybdenum, the two peaks at 230.4 and 232.5 eV were attributed respectively to MoO_xS_y (17%) and Mo-oxide (77%).

In summary, the comparison between S2p and Mo3d spectra recorded on the IF-MoS_2 powder and the ubetched Fuchs 5W30 + MoS_2 tribofilm indicates that both molybdenum and sulfur

TABLE 4—XPS QUANTIFICATION OF TRIBOFILMS OBTAINED WITH FUCHS 5W30 + MoS_2, AT THE UPPERMOST SURFACE AND AFTER 0.2, 1, 4, 10, AND 18 MIN OF ETCHING

Elemental Composition (at%)	Top Surface	0.2 min of Etching	1 min of Etching	4 min of Etching	10 min of Etching	18 min of Etching
C1s	49	23.5	16.5	14.5	13	9.9
O1s	35	50	52	49	40	15
Ca2p	9.5	16	19	19.2	15	2.9
P2p	1.6	2.6	2	1.8	0.4	0
S2p	2.3	2.6	2.2	2	1.8	0.4
Mo3d	2.1	3.8	4.5	4	3.5	0.8
Fe2p	0	1.5	3.8	9.5	26.3	71
Total	100	100	100	100	100	100

were mainly found in an oxidized form in the uppermost surface of the tribofilm.

After etching, an increase in the intensity of the S-Mo bonds can be observed in both S2p and Mo3d peaks. In contrast, the intensities of the S−O and Mo−O bonds decrease progressively with etching time. This suggests that the oxidation of the tribofilm mainly occurred after the engine test due to the air atmosphere.

With regard to the sulfur, a new contribution is observed after 0.2, 4, and 10 min of etching at, respectively, 160.4, 159.5, and 159.9 eV, indicating the presence of sulfide in the tribofilm (Moulder, et al. *(10)*).

The binding energies of the peak corresponding to the S−Mo bond were shifted to low binding energy after etching compared to the uppermost surface. This shift could be explained by the

TABLE 5—BINDING ENERGIES AND CORRESPONDING CHEMICAL SPECIES OF S2P, MO3D, C1S, O1S AND FE2P PEAKS OF XPS SPECTRA OBTAINED FROM THE IF-MoS_2 POWDER AND FROM THE TRIBOFILM FORMED WITH FUCHS 5W30 + MoS_2 BEFORE ETCHING AND AFTER 0.2, 1, 4, 10, AND 18 MIN OF ETCHING

	Binding Energies, Chemical Species, and Concentrations				
Elements	S2p Peaks	Mo3d Peaks	C1s Peaks	O1s Peaks	Fe2p Peaks
Top surface	161.90 eV, MoS_2, 25% 163.00 eV, sulfur, C−S, 5% 167.00 eV, S−O, 17% 168.90 eV, S−O, 53%	229.10 eV, MoS_2, 5% 230.40eV, MoO_xS_y, 17% 232.50 eV, Mo−O, 77% S2s, 1%	284.80 eV, C−C, 70% 286.35 eV, C−O, C−S, 20% 289.80 eV, $CaCO_3$, 10%	531.40, S−O/Mo−O/$CaCO_3$, 70% 532.80, O−C, 30%	……
After 0.2 min of etching	160.40 eV, sulfides, 40% 161.50 eV, S−Mo/S−Fe, 29% 165.90 eV, S−O, 10% 167.60 eV, S−O, 20%	228.8 eV, Mo−S, 28% 231.3 eV, MoO_xS_y, 70% S2s, 2%	282.80 eV, carbides, 45% 284.75 eV, C−C, 26% 287.80 eV, C−O, 28%	528.65, oxide, 49% 530.45, Mo−O, 51%	709.70, Fe−S/Fe−O, 20% 711.60, Fe−OH, 50% 713.90, Fe−S−O, 30%
After 1 min of etching	159.60, sulfides, 55% 161.60, S−Mo/S−Fe, 35% 165.65, S−O, 2% 167.60 eV, S−O, 8%	228.9 eV, Mo−S, 35% 231.2 eV, MoO_xS_y, 63% S2s, 2%	282.65 eV, carbides, 33% 284.35 eV, C−C, 17% 286.60 eV, S−C−S, 24% 288.60 eV, C−O, 25%	528.50, oxide, 44% 530.40, Mo−O, 41%	708.00, Fe−O, 40% 710.40, Fe^{3+}/Fe−S, 40% 712.90, Fe−S−O, 20%
After 4 min of etching	159.50 e V, sulfides, 57% 161.60 eV, S−Mo/S−Fe, 38% 166.80 eV, S−O, 2% 168.25 eV, S−O, 5%	229 eV, Mo−S, 37% 231.20 eV, MoO_xS_y, 61% S2s, 2%	282.65 eV, carbides, 30% 284.40 eV, C−C, 23% 286.60 eV, S−C−S, 31% 288.80 eV, C−O, 16%	528.50, oxide, 42% 530.50, Mo−O, 45%	707.00, Fe°/Fe−S, 59% 708.50, Fe−O, Fe^{2+}, 20% 710.15, Fe−S/Fe−O, 13% 712.05, Fe−S−O, 8%
After 10 min of etching	159.90 eV, sulfides, 10% 161.75 eV, S−Mo/S−Fe, 90%	228.4 eV, Mo−S 25% 231 eV, MoO_xS_y, 55% 232.9 eV, Mo−O, 19% S2s 1%	282.95 eV, carbides, 36% 284.35 eV, C−C, 17% 286.75 eV, S−C−S, 34% 289.10 eV, $CaCO_3$, 13%	528, oxide, 50% 529.80, Mo−O, Fe−O, 50% 531.65, O−C, Fe−S−O, 26%	707.05, Fe°/Fe−S, 65% 708.50, Fe−O, Fe^{2+}, 20% 710.15, Fe−S/Fe−O, 11% 712.10, Fe−S−O, 4%
After 18 min of etching	161.82 eV, S−Mo/S−Fe, 95% 168.60 eV, S−O, 5%	228.4 eV, Mo−S, 40% 230.10 eV, MoO_xS_y, 30% 232.10 eV, Mo−O, 15% 233.50 eV, Mo−O, 15% S2s, 3%	283.35 eV, carbides, 31% 285.00 eV, C−C, 10% 287.35 eV, C−O, 51% 289.45 eV, $CaCO_3$, 6%	528.50eV, oxide, 8% 529.80 eV, Fe−O, Mo−O, 50% 531.50 eV, C−O/S−O/Mo−O, $CaCO_3$, 42%	707.00, Fe°/Fe−S 70% 708.50, Fe−O, Fe^{2+}, 20% 710.15, FeS/FeO, 8% 712.10, Fe−S−O, 2%

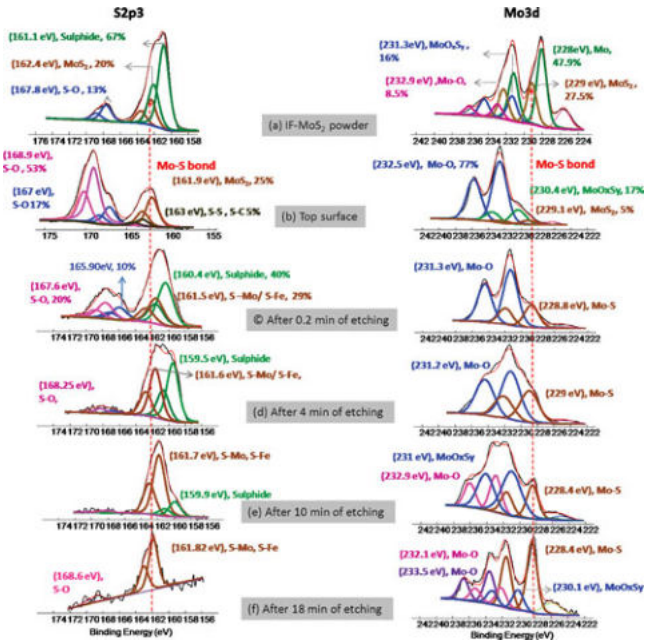

Fig. 8—Fitted Mo3d and S2p XPS spectra of (a) IF-MoS_2 powder, (b) Fuchs 5W30 + MoS_2 tribofilm, (c) Fuchs 5W30 + MoS_2 tribofilm after 0.2 min of etching, (d) Fuchs 5W30 + MoS_2 tribofilm after 4 min of etching, (e) Fuchs 5W30 + MoS_2 tribofilm after 10 min of etching, and (f) Fuchs 5W30 + MoS_2 tribofilm after 18 min of etching.

presence of small quantities of iron sulfide species in the tribofilm formed either from the sulfur remaining from the synthesis process and/or from the chemical reaction between the S atoms of the sheets of MoS_2 coming from the exfoliation process of the fullerenes and the Fe atoms (Tannous, et al. *(12)*). Moreover, the peaks corresponding to S−O bonds become negligible after 1 min of etching (Table 5). This indicates that the sulfur was mainly bonded with molybdenum (S−Mo bond) and/or with iron (S-Fe) in the tribofilm after etching.

Whereas before etching, the major Mo3d peak was found at 232.5 eV corresponding to the Mo−O bond (78%), after etching the two major Mo3d peaks were in the range of 228.4–229 eV and 230.1–231.3 eV. This suggests that in depth, the molybdenum remained in the form of MoS_2 and MoO_xS_y.

The binding energies of the O1s peak were between 528.5 and 531.5 eV, suggesting the presence of oxide species in the tribofilm (O−S, O−Mo, O−Fe, O−P, O−Ca); however, it was not evident to distinguish the contribution of each oxide species.

The binding energies of the fitted Fe2p peaks show that iron was found in form of Fe−S/Fe−S−O/Fe−O in the tribofilm, after 0.2 and 1 min of etching (Table 5). A peak at 707 eV appears after 4 min of etching. This peak could be attributed to Fe metal and/or Fe−S bonds.

It can also be seen from Table 5 that after etching, the major portion of carbon remaining on the tribofilm was oil containing CS_2, $CaCO_3$, and hydrocarbon species.

In summary, based on XPS depth analysis, it was shown that a tribofilm was formed inside the contact area of the RFF when lubricated with the Fuchs 5W30 + MoS_2 oil. This tribofilm could explain the observed improved antifriction properties of the lubricant containing the nanoparticles. Indeed, the contribution of the IF-MoS_2 nanoparticles to the formation of this tribofilm was clearly proved. Though molybdenum and sulfur were mainly oxidized at the uppermost surface of tribofilm, they remained in the form of MoS_2 and MoO_xS_y in depth.

In the present study, no systematic quantification of wear rates was possible. On the other hand, the antiwear properties of a lubricant are not always directly correlated to the antifriction effect (and, in some cases, improved antifriction behavior is combined with an improved wear rate). For this reason, the possible wear protection related to the addition of IF-MoS_2 powder in the oil deserves more attention and will be the object of future studies.

CONCLUSION

A fully formulated zinc-free engine oil containing nanoparticles was developed and tested on a full engine subsystem mimicking the real tribological conditions encountered by the lubricant in the valve-train and engine head. An accelerated annealing program was applied to evaluate the behavior of the oil over an extended time of usage. The bench tests revealed an important contribution of the MoS_2 nanoparticles in reducing the coefficient of friction in all lubrication regimes. The effect of nanoparticles became evident after some hours of testing, suggesting that the mechanism of action is related to the formation, assisted by the mechanical exfoliation action, of a tribofilm on the contact surfaces.

XPS analysis gave a further confirmation of this hypothesis: the presence of molybdenum and an increased quantity of sulfur in the wear tracks obtained with the lubricant containing nanoparticles can be correlated to the formation of a tribolayer composed of Mo and S. The formation of a tribolayer could protect the surfaces and improve the antiwear properties of the lubricant. These aspects deserve further investigation.

In conclusion, a stable fully formulated nanolubricant, showing improved antifriction properties in comparison with the standard additive package, was produced and tested in a relevant environment for internal combustion engines applications. Because the engine head bench test was an unfired apparatus, the testing procedure was not able to take into account the effect of nanoparticles on an oxidizing atmosphere commonly present in internal combustion engines. The qualification of the nanolubricant in real engines will be the object of a successive publication.

FUNDING

This work was supported by EU seventh framework program ADDNANO (FP7-NMP-2008-LARGE-2 Project No. 229284).

REFERENCES

(1) Cizaire, L., Vacher, B., Le Mogne, T., Martin, J. M., Rapoport, L., Margolin, A., and Tenne, R. (2002), "Mechanisms of Ultra-Low Friction by Hollow Inorganic Fullerene-Like MoS_2 Nano-Particles," *Surface Coating Technology*, **160**, pp 282–287.

(2) Joly-Pottuz, L., Dassenoy, F., Belin, M., Vacher, B., Martin, J. M., and Fleischer, N. (2005), "Ultralow-Friction and Wear Properties of IF-WS_2 under Boundary Lubrication," *Tribology Letters*, **18**, pp 477–485.

(3) Lahouij, I., Dassenoy, F., Vacher, B., and Martin, J. M. (2012), "IF-MoS_2 Based Lubricants: Influence of Size, Shape and Crystal Structure," *Wear*, **296**, pp 558–567.

(4) Yadgarov, L., Petrone, V., Rosentsveig, R., Feldman, Y., Tenne, R., and Senatore, A. (2013), "Tribological Studies of Rhenium Doped Fullerene-Like MoS_2 Nano-Particles in Boundary, Mixed and Elasto-Hydrodynamic Lubrication Conditions," *Wear*, **297**, pp 1103–1110.

(5) Verma, A., Jiang, W., Safe, H. H. A., Brown, W. D., and Malshe, A. P. (2008), "Tribological Behavior of Deagglomerated Active Inorganic Nano-Particles for Advanced Lubrication," *Tribology Transactions*, **51**(5), pp 673–678.

(6) Gullac, B. and Akilin, O. (2010), "Frictional Characteristics of IF-WS2 Nano-Particles in Simulated Engine Conditions," *Tribology Transactions*, **53**(6), pp 939–947.

(7) Mosleh, M. and Ghaderi, M. (2012), "Deagglomeration of Transfer Film in Metal Contacts Using Nanolubricants," *Tribology Transactions*, **55**(1), pp 52–58.

(8) Morina, A., Neville, A., Priest, M., and Green, J. H. (2006), "ZDDP and MoDTC Interactions and Their Effect on Tribological Performance—Tribofilm Characteristics and Its Evolution," *Tribology Letters*, **24**(3), pp 243–256.

(9) Utomo, A., Addison, T., Konan, G., and Ozcan-Taskin, G. (2013), "Milling of Nanoparticle Clusters for New Formulation Lubricants," *Nanotech 2013: Technical Proceedings of the 2013 NSTI Nanotechnology Conference and Expo*, CRC Press [CD-ROM].

(10) Moulder, J. F., Stickle, W. F., Sobol, P. E., and Bomben, K. D. (1992), *Handbook of X-ray Photoelectron Spectroscopy*, 2nd ed., Waltham, MA: Perkin-Elmer Corporation.

(11) Jenei, I., Svahn, F., and Csillag, S. (2013), "Correlation Studies of WS_2 Fullerene-Like Nanoparticles Enhanced Tribofilms: A Scanning Electron Microscopy Analysis," *Tribology Letters*, **51**, pp 461–468.

(12) Tannous, J., Dassenoy, F., Lahouij, I., Le Mogne, T., Vacher, B., Bruhacs, A., and Tremel, W. (2011), "Understanding the Tribochemical Mechanism of IF-MoS_2 Nano-Particles under Boundary Lubrication," *Tribology Letters*, **41**, pp 55–64.